Waring, M. J., Wakelin, L. P. G., & Lee, J. S. (1975) *Biochim. Biophys. Acta 407*, 200–212.
Wells, R. D., & Wartell, R. M. (1974) in *Biochemistry of Nucleic Acids* (Kornberg, H. L., Phillips, D. C., & Burton, K., Eds.) Vol. 6, pp 41–64, University Park Press, Baltimore, MD.
Wilson, D. W., Grier, D., Reinier, R., Baumann, J. D., Preston, J. F., & Gabbay, E. J. (1976) *J. Med. Chem. 19*, 381–384.

Interaction of Crystal Violet with Nucleic Acids†

L. P. G. Wakelin,‡ A. Adams, C. Hunter, and M. J. Waring*

ABSTRACT: Sedimentation and viscosity experiments reveal that when crystal violet binds to closed circular deoxyribonucleic acid (DNA) the helix becomes unwound. The average angle of unwinding per bound dye molecule is 9.8 ± 0.6°. Viscosity measurements with sonicated rodlike fragments of calf thymus DNA provide evidence that the binding causes an apparent decrease in contour length. Scatchard plots for binding to DNA are curvilinear, concave upward, indicative of strong exclusion effects and/or heterogeneity of binding sites having different affinity. By contrast, binding curves for RNA are curvilinear, concave downward, suggestive of cooperativity. Crystal violet binds preferentially to DNA, its intrinsic association constant being 15-fold lower for ribonucleic acid (RNA) at ionic strength 0.01 and 46-fold lower in 0.2 M salt solution. Heat denaturing DNA radically alters the binding mechanism such that Scatchard plots acquire the "humped" appearance characteristic of a cooperative reaction. Its preference for binding to helical DNA is confirmed by a large increase in the "melting" temperature of calf thymus DNA in buffer of low ionic strength. Raising the ionic strength decreases affinity constants generally, and at a salt concentration of 0.75 M binding to secondary sites on DNA is substantially reduced. Temperature-jump measurements reveal two fast closely coupled relaxation times at low levels of binding whereas at higher binding ratios an additional two exponential components can be resolved, again closely coupled but well separated from the fast effects. Thus, the ligand forms at least two distinct complexes with DNA at low levels of binding, and there are not less than four bound species at higher binding ratios. The visible absorption spectrum of the crystal violet–DNA complex becomes increasingly bathochromic and hypochromic as the binding ratio is raised. However, the spectrum of the dye bound to RNA is characterized by a strong hypsochromic component and a much greater hypochromism at higher binding ratios than is seen with DNA. These spectral properties are attributed to changes in the propeller-like conformation of the dye due to rotations which affect the relative disposition of the phenyl rings and/or their dimethylamino substitutents.

Studies of the interaction between triphenylmethane dyes and deoxyribonucleic acid (DNA)[1] have produced conflicting accounts of the mechanism of binding (Lerman, 1961, 1964 a,b; Neville & Davies, 1966; Armstrong & Panzer, 1972; Müller & Gautier, 1975). Lerman (1961, 1964a) reported that these dyes increase the viscosity of DNA to an extent comparable to that found for acridines, which led him to propose that both types of ligand intercalate. He also found that on binding to DNA there was a marked decrease in the reactivity of the amino groups of pararosaniline; this he offered as further evidence that the cation is at least partially buried within the helix (Lerman, 1964b). Armstrong & Panzer (1972) confirmed the increase in viscosity up to r (moles of dye bound per mole of DNA phosphate) = 0.1 and suggested that pararosaniline intercalates so as to exclude similar binding at the three nearest-neighbor sites on either side of a bound dye molecule. In addition, they identified a second form of binding at $r > 0.125$ which did not affect viscosity and which they postulated to involve external attachment to the surface of the DNA helix. In contrast to these reports, X-ray diffraction studies on pararosaniline–DNA fibers did not reveal the intercalation-induced changes in layer-line spacing observed with acridine–DNA complexes (Neville & Davies, 1966). Similarly, Müller & Gautier (1975) found only very small effects of crystal violet on the viscosity and sedimentation coefficient of sonicated rodlike fragments of DNA which, although tending in the correct direction, were considered far too small to be compatible with an intercalation process. They concluded that crystal violet binds externally and that the dye, in addition to having a general nonspecific affinity for DNA, interacts preferentially with two adjacent A-T base pairs. They further surmised that the base pair selective interaction exhibits exclusion effects whereas the nonspecific binding is cooperative (Müller & Gautier, 1975).

The crystal structure of triphenylmethyl perchlorate shows the carbonium ion as a symmetrical propeller-shaped molecule with three coplanar central bonds bearing the aromatic rings inclined at an angle of 54° to one another (Gomes de Mesquita et al., 1965). NMR evidence confirms that this propeller configuration almost certainly pertains in solution (Moodie et al., 1959; Olah, 1964; Farnum, 1964, 1967; Schuster et al., 1968). This nonplanar conformation contrasts with that of the established fused-ring aromatic intercalating agents, and it might therefore be supposed that intercalation of the carbonium ion is precluded on steric grounds. A further feature which distinguishes triphenylmethane dyes from classical in-

† From the Department of Pharmacology, University of Cambridge Medical School, Cambridge, CB2 2QD, England. *Received March 5, 1981.* We acknowledge the support of a Medical Research Council Training Fellowship and a Science Research Council Research Assistantship (L.P.G.W.). Purchase of equipment and supplies was aided by grants from the Science Research Council, the Medical Research Council, the Royal Society, and the Cancer Research Campaign.

‡ Present address: The Cancer Institute, Peter MacCallum Hospital, Melbourne, Victoria 3000, Australia.

[1] Abbreviations used: DNA, deoxyribonucleic acid; RNA, ribonucleic acid; Hepes, 4-(2-hydroxyethyl)-1-piperazineethanesulfonic acid; EDTA, ethylenediaminetetraacetic acid; Mes, 2-(*N*-morpholino)ethanesulfonic acid.

0006-2960/81/0420-5779$01.25/0

tercalating agents is their tendency to concentrate residual charge on the para substituent which results, in the case of crystal violet, in a symmetrical array of basic centers (Ray et al., 1971). This pattern of charges might well predispose the ligand molecule to interact with DNA by some novel, nonintercalative mechanism(s).

In this paper we report the results of hydrodynamic experiments with circular DNA and sonicated rodlike fragments of DNA, aimed at resolving the conflicting reports concerning the intercalation potential of triphenylmethane dyes. We have further characterized the binding reaction by employing equilibrium dialysis to determine the relative affinity of crystal violet for DNA, RNA, and heat-denatured DNA. Temperature-jump and visible absorption spectroscopy have been used to delineate more clearly the multifarious bound forms of the dye revealed by the equilibrium binding studies.

Experimental Procedures

Materials

Buffers. Experiments were conducted in Hepes–NaOH buffers, pH 7.0, at room temperature (designated SHE buffers) containing 2 mM Hepes (Calbiochem), 10 μM EDTA, and NaCl to yield the required ionic strength (9.4, 49.4, and 199.4 mM to give ionic strengths 0.01, 0.05, and 0.20, respectively) and an Mes–NH_4F buffer which contained 2 mM Mes, 10 μM EDTA, and 0.75 M NH_4F adjusted to pH 6.0 at 25 °C with ammonia solution. Reagent grade water from a Millipore Milli-Q2 system was used throughout.

Nucleic Acids. Bacteriophage PM2 DNA was prepared by the method of Espejo et al. (1969) using strains of virus and host bacteria kindly provided by Dr. R. T. Espejo. Samples used in viscometric titrations were free of nicked circular molecules as judged by analytical ultracentrifugation, whereas samples for use in ultracentrifugal titrations contained 20–30% of the nicked circular species generated by repeated freezing and thawing. Calf thymus DNA (highly polymerized sodium salt, type 1) was purchased from Sigma Chemical Co. Solutions containing 2 mg/mL were prepared by gently homogenizing the DNA together with 0.01 SHE buffer until dissolved; they were dialyzed extensively against buffer of the required ionic strength, clarified by filtration through two Whatman GF-C glass fiber filters, and stored frozen at −22 °C. PM2 and native calf thymus DNA concentrations were determined by assuming a molar extinction coefficient at 260 nm of 6600 per nucleotide. Heat-denatured calf thymus DNA was prepared by heating a solution in 0.01 or 0.20 SHE buffer at 100 °C for 20 min and then cooling rapidly to 0 °C in an ice–water bath. Molar extinction coefficients at 260 nm of 8270 and 8180 at room temperature were determined in 0.01 and 0.20 SHE buffers, respectively. High molecular weight whole yeast RNA was obtained from Calbiochem-Behring Corp., and solutions of it were prepared in the manner described above for calf thymus DNA. RNA concentrations were determined by using an assumed molar extinction coefficient at 260 nm of 8500. Denatured DNA and RNA solutions were dialyzed exhaustively for 3 days at 4 °C against the experimental buffer by using Visking dialysis tubing of nominal molecular weight cutoff 12 000 to ensure that low molecular weight material was removed from the samples prior to use in binding studies.

Crystal Violet. The dye was provided as the hydrated chloride salt by Dr. G. W. Grigg, C.S.I.R.O. Molecular and Cellular Biology Unit, North Ryde, N.S.W. 2113, Australia. Its purity was verified by NMR measurements which showed that the sample contained 0.75 mol of water/mole of dye. The solid material was stored in a desiccator in the dark at 0–4 °C, and solutions were freshly prepared or stored frozen at −22 °C. Siliconized glassware was used throughout to minimize losses by adsorption to glass surfaces. Molar extinction coefficients in the experimental buffers and buffer–dimethyl sulfoxide (Me_2SO) mixtures were measured by direct weighing in the concentration range 1–10 μM (see Table I). At ionic strength 0.75 the dye adsorbed even to siliconized glassware and to quartz optical cuvettes. This problem was circumvented by addition of dimethyl sulfoxide to a final concentration of 10% (v/v) before measuring the absorption of samples.

Methods

Analytical Ultracentrifugation. Sedimentation coefficients were measured by boundary sedimentation at 20 °C and 34 000 rpm in a Beckman Model E ultracentrifuge equipped with ultraviolet optics. Details of procedures and computation of s_{20} values were as previously described (Waring, 1970). Crystal violet–DNA complexes were prepared by method 2 of Waring (1970) in which successive increments of dye solution in buffer are added directly to an ultracentrifuge cell containing 0.600 mL of PM2 DNA in buffer having an absorbance at 260 nm of 0.600 (i.e., 91 μM in nucleotides). In all cases the crystal violet and DNA were in contact for at least 30 min before commencement of sedimentation, a period which assures adequate attainment of equilibrium (see Results). Sedimentation coefficients are presented as directly determined; they were not corrected for viscosity, buoyancy, or DNA concentration.

Viscometry. Measurements using closed circular PM2 DNA were performed essentially according to the method of Revet et al. (1971) as described by Waring & Henley (1975) by using a simple viscometer having a 10-cm capillary of 0.4-mm bore and a bulb of volume 0.7 mL, thermostated at 20 ± 0.01 °C. The flow time for water was 104.0 s. For routine experiments the viscometer contained 1.0 mL of a 303 μM solution of PM2 DNA (OD_{260} = 2.00; flow time 111.7 s). Crystal violet was added in increments of 1–20 μL from a Burkard precision micrometer syringe of 1-mL volume via a fine plastic tube inserted down the ascending limb of the viscometer; after each addition complete mixing was effected by bubbling a gentle current of air down the ascending limb. The syringe and tube were thoroughly soaked in crystal violet solution prior to use to minimize losses of material by adsorption to glass and plastic surfaces. Even so, the actual concentration of the dye solution delivered from the tip of the plastic tube was always determined before and after each experiment by visible absorption measurements, aliquots of dye solution being diluted 1:200 (v/v) in glacial acetic acid. Solutions were freed of particulate material by centrifuging for 15 min at 4000 rpm before use. Flow times were measured in triplicate to an accuracy of 0.1 s; the average deviation of a set of measurements was 0.1–0.2 s, i.e., ~0.1%. No kinetic effects attributable to the rate of complex formation were detected. Reduced viscosities η_{red} were calculated by established methods, taking into account the dilution caused by the addition of the crystal violet solution (Revet et al., 1971; Waring & Henley, 1975; Wakelin et al., 1978).

For experiments designed to measure the helix extension produced by binding of crystal violet, calf thymus DNA was sonicated to fragments of molecular weight (3–5) × 10^5 (Crothers & Zimm, 1965) as previously described (Wakelin & Waring, 1976). Viscometric measurements on this DNA were performed essentially by the method of Cohen & Eisenberg (1966, 1969) using a simple viscometer having a 10-cm capillary of 0.4-mm bore and a bulb of volume of 1.5 mL, again thermostated at 20 ± 0.01 °C. The viscometer contained

Table I: Formula and Molar Extinction Coefficients

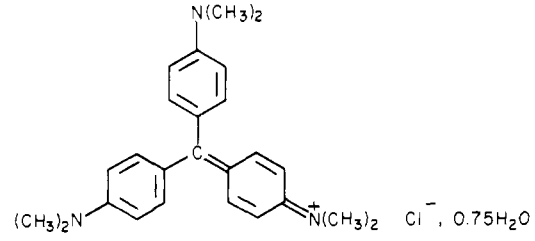

solvent	extinction coeff: buffer	extinction coeff: 50% Me_2SO–buffer mixture
0.01 SHE	$\epsilon_{590} = 8.74 \times 10^4$	$\epsilon_{598} = 9.85 \times 10^4$
0.20 SHE	$\epsilon_{590} = 9.05 \times 10^4$	$\epsilon_{598} = 9.84 \times 10^4$
0.75 NH_4F-Mes	ϵ_{590} [a] $= 8.53 \times 10^4$	$\epsilon_{598} = 9.52 \times 10^4$
glacial acetic acid	$\epsilon_{589} = 12.06 \times 10^4$	

[a] Buffer contained 10% Me_2SO.

1.8 mL of a 606 μM solution of sonicated DNA to which crystal violet was added in the manner described above. In these experiments the amount of crystal violet delivered through the plastic tube was monitored by measuring the absorption of aliquots diluted with the experimental buffer. The data were transformed directly from flow times to values for the relative contour length as described previously (Wakelin et al., 1978) by using the equation

$$\frac{L}{L_0} = \left[\frac{t_c - t_0(v)}{t_d - t_0(v)}\right]^{1/3}$$

using where L is the contour length in the presence of crystal violet, L_0 is the contour length of free DNA, t_c is the flow time for the complex, t_d is the flow time for pure DNA, and $t_0(v)$ is the flow time for buffer at a given total volume, v, in the viscometer. This equation assumes that hydrodynamic interaction effects such as are occasionally encountered for polyelectrolytes at low ionic strength may be neglected in calculating L/L_0 from viscometric data, as concluded in earlier studies using essentially the same methodology (Reinert, 1972; Waring & Wakelin, 1974; Balcarova et al., 1978; Wakelin et al., 1978).

Equilibrium Dialysis. Binding curves were measured by equilibrium dialysis using an M.S.E Dianorm apparatus. Dialysis cells having either two 5-mL or two 1-mL compartments separated by a Spectrapor 3 regenerated cellulose membrane (nominal molecular weight cutoff 3500–4500) were loaded with 4 or 1 mL of nucleic acid solution in the concentration range 91–606 μM in one chamber and an equal volume of crystal violet solution in the other. The cells were rotated to establish equilibrium in a water bath at 20 or 25 °C for 20 h, after which time the dye concentration in each chamber was determined spectrophotometrically in 40- or 10-mm light path semimicro quartz cuvettes. For the free dye side the molar extinction coefficients determined by direct weighing were used (see Table I); for the other side the complex was dissociated by addition of an equal volume of dimethyl sulfoxide (Me_2SO), and the total dye concentration was estimated by using molar extinction coefficients determined for 50% (v/v) buffer–Me_2SO mixtures, also listed in Table I. Appropriate controls were performed to verify complete dissociation of the crystal violet complexes by Me_2SO over the entire range of binding levels studied, to establish that no nucleic acid leaked across the membrane under the conditions of the experiment and to ensure attainment of equilibrium within the 20-h period of rotation. Additional checks were made to monitor nonspecific losses of ligand due to binding to cells and membranes, but since the total concentration of crystal violet in solution in each chamber was determined by direct measurement, no corrections need be applied. The concentration of bound ligand, equal to the difference between total and free drug concentrations (c), was divided by the nucleic acid concentration to yield the binding ratio r (moles of drug bound per mole of nucleotides), and equilibrium isotherms were constructed in the form of Scatchard plots (r/c vs. r).

Equilibrium dialysis was also used to determine the absorption spectrum of bound crystal violet as a function of the binding ratio for complexes with DNA, denatured DNA, and RNA. In these experiments the difference spectrum between the solutions in the free dye side and the complex-containing compartment was measured by using a Unicam SP8-200 recording spectrophotometer, and the binding ratio subsequently was determined by dissociation of the complex with Me_2SO as described above. Spectra of complexes were normalized by dividing the measured absorbance by the concentration of bound ligand to yield plots of extinction coefficient vs. wavelength.

Thermal Denaturation Profiles. "Melting" curves for calf thymus DNA–crystal violet complexes were measured by using the Unicam SP8-200 spectrophotometer equipped with an automatic sample changer containing a water-jacketed cell holder, so that four samples could be examined in a single experiment (Waring & Henley, 1975; Lee & Waring, 1978). Four Teflon-stoppered quartz cuvettes of 10-mm light path and 3-mL capacity were employed; one contained a thermistor probe, the resistance of which was continuously monitored to provide a direct measurement of the temperature of the liquid inside the cuvettes. The temperature of the cell holder was raised by a Haake circulating water bath with its contact thermometer driven by a synchronous electric motor to produce a temperature rise of 0.6 °C/min. The absorbance at 260 nm was monitored for each sample, and the melting temperature, T_m, was taken as the midpoint of the hyperchromic transition.

Temperature-Jump Relaxation Spectrometry. Temperature-jump difference spectra of crystal violet–DNA complexes were measured by using the apparatus described by Wakelin & Waring (1980). The temperature rise, achieved by Joule heating, was mediated by discharge of a 0.05-μF capacitor at 30 kV into a Teflon cell with a heated volume of 0.8 mL and an optical path length of 10 mm. The high-voltage discharge resulted in a temperature increase of 6.5 °C with an experimental response time limited at high ionic strength by the photomultiplier rise time of 2–3 μs. The optical signal was recorded on a Datalab DL905 transient recorder and displayed on a Tektronix Model 5103N oscilloscope. The photomultiplier was offset at 5.0 V, making a 1-mV signal equivalent to an absorbance change of 8.7×10^{-5}. Relaxation times were determined by using a nonlinear least-squares Gauss–Newton method (Johnson & Schuster, 1974) as previously described (Wakelin & Waring, 1980).

Results

Sedimentation and Viscosity Measurements. Crystal violet removed and reversed the supercoiling of PM2 DNA in a decisive fashion as illustrated in Figure 1a. The equivalence input ratio (molar ratio of total added drug to DNA nucleotides which causes complete relaxation of supercoiling) was 0.185 ± 0.050 in buffer of ionic strength 0.01 (Figure 1a). This ratio was corrected to a binding ratio (r) of 0.135 ± 0.035 by using a binding curve determined for calf thymus DNA under identical ionic conditions (see Figure 3a and Table II).

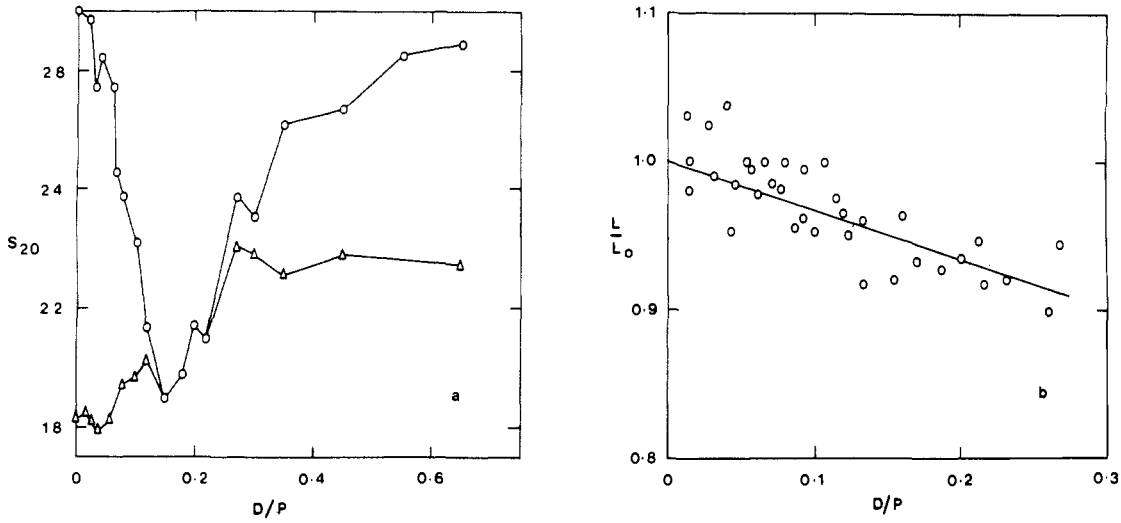

FIGURE 1: Effects of crystal violet on the sedimentation coefficient of PM2 DNA and on the relative contour length of sonicated calf thymus DNA. In (a) the S_{20} of closed circular duplex molecules is represented by circles; that of the nicked circular molecules is shown as triangles; when both components cosedimented as a single unresolved boundary only the circular symbol is plotted, representing the weight-average sedimentation coefficient for both species together. The abscissa shows the input ratio; i.e., the molar ratio of added dye to DNA nucleotides. In (b) the ordinate represents the calculated ratio of contour lengths in the presence (L) or absence (L_0) of the ligand. The solvent was 0.01 SHE buffer, pH 7.0, at 20 °C.

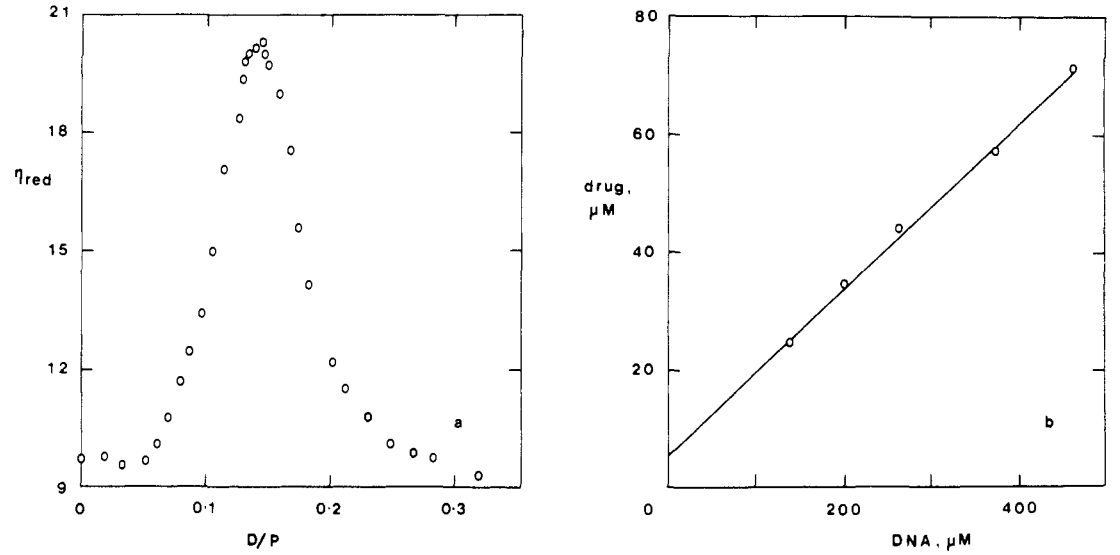

FIGURE 2: Titration of the supercoiling of PM2 DNA by crystal violet. (a) Effect on the viscosity in 0.01 SHE buffer, pH 7.0, at 20 °C. The initial DNA concentration was 303 μM. The ordinate represents the reduced viscosity in dL/g; the abscissa shows the molar ratio of added dye to DNA nucleotides. In (b) the ordinate and abscissa show, respectively, the absolute concentrations of total crystal violet and DNA in the viscometer at the maximum of reduced viscosity plots like that presented in (a). For the different experiments the starting DNA concentration was varied between 150 and 500 μM in nucleotides. Measurements were made in SHE buffer of ionic strength 0.05 at pH 7.0 and 20 °C.

the correction assumes that contributions from the free energy of supercoiling to the effective association constant vanish for fully relaxed circles and that the intrinsic binding parameters are the same for these two DNAs of equal base composition. The experiment yields a helix unwinding angle of 9.8 ± 3.5°, taking that of ethidium to be 26° (Wang, 1974; Wakelin & Waring, 1974; Keller, 1975). An unusual feature of Figure 1a is the increase in sedimentation coefficient of the nicked circular molecules at higher binding ratios: classical intercalators cause a decrease in S_{20} of this component (Waring, 1970; Wakelin & Waring, 1974).

Changes in contour length of the DNA helix associated with binding of crystal violet were investigated as in Figure 1b, which reveals a steady decrease in contour length as the level of dye binding rises. In this low-salt buffer more than 90% of the added dye is bound at an input ratio of 0.25, and the L/L_0 plot is well described by a straight line of slope $-0.33r$. Thus, while the effect of crystal violet on the supercoiling of PM2 DNA is characteristic of intercalating agents, its effect on the sedimentation coefficient of nicked circular DNA (which approximates the behavior of linear DNA) and its ability to decrease the contour length of sonicated DNA are not consistent with a simple intercalative mode of binding.

Viscometric titrations using supercoiled DNA were undertaken in order to substantiate the helix-unwinding effect of crystal violet. Figure 2a shows the result of an experiment performed under solvent conditions identical with those used in the sedimentation experiments. In this instance, however, the DNA solution was considerably more concentrated (303 μM), and the equivalence input ratio occurs at 0.140. The response is comparable to that seen with ethidium in regard to the shape of the curve and the reduced viscosity of the relaxed circular DNA complex (Waring & Henley, 1975). To determine the true equivalence binding ratio, we determined the position of the equivalence peak at a range of DNA concentrations. However, it proved necessary to increase the ionic

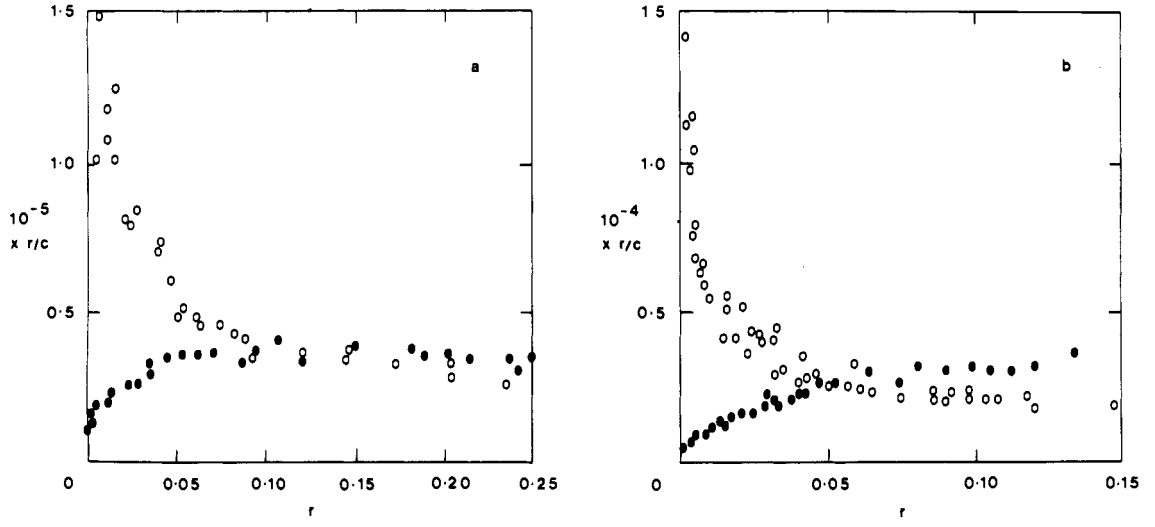

FIGURE 3: Interaction between crystal violet and calf thymus DNA (○) and wheat germ RNA (●). The data are plotted according to Scatchard (1949), where r is the binding ratio (drug molecules bound per nucleotide) and c is the free ligand concentration. In (a) the buffer was 0.01 SHE, pH 7.0, at 20 °C; in (b) the ionic strength was increased to 0.2.

strength of the buffer to 0.05 to prevent precipitation of the drug–DNA complex at the high DNA concentrations required in these experiments. In Figure 2b the concentration of crystal violet required to relax the supercoiling of the circles is plotted as a function of the DNA concentration. For a simple mass-action interaction, such a plot should take the form of a straight line with a slope equal to the equivalence binding ratio and an intercept on the ordinate equal to the free drug concentration in equilibrium with the relaxed circular DNA complex (Revet et al., 1971; Waring & Henley, 1975). The data in Figure 2b reveal that this condition is satisfactorily met and yield an equivalence binding ratio of 0.138 ± 0.008, corresponding to a helix unwinding angle of 9.8 ± 0.6°. Thus, the two independent determinations of the helix unwinding capacity of crystal violet give experimentally indistinguishable results. It is also evident that the unwinding angle is not affected by raising the ionic strength from 0.01 to 0.05.

Equilibrium Binding and Thermal Denaturation Measurements. Figure 3a shows Scatchard plots for crystal violet binding to DNA and RNA in buffer of ionic strength 0.01. Neither nucleic acid yielded binding data amenable to simple Scatchard analysis nor could the results be fitted by eq 10 of McGhee & Von Hippel (1974) which corresponds to an excluded-site model. In the case of DNA the data are curvilinear (concave upward) indicative of marked anticooperativity and/or heterogeneity of binding sites having differing affinities (Crothers, 1968; Gurskii et al., 1972; McGhee & Von Hippel, 1974). In this situation the intrinsic association constant to an isolated potential binding site, $K_{(0)}$, can be estimated by extrapolating to the ordinate axis (Crothers, 1968; Müller & Crothers, 1968; McGhee & Von Hippel, 1974), yielding a value of $K_{(0)}$ for DNA of 1.5×10^5 M^{-1} (Table II). However, no sensible estimate for the binding site size can be made. By contrast, the results for RNA (Figure 3a) are just the converse of those described for DNA with the Scatchard plot being curvilinear concave downward, strongly suggestive of cooperative binding (Crothers, 1968; Gurskii et al., 1972; McGhee & Von Hippel, 1974). Although precipitation of the drug–RNA complex limited the accessible range of binding, precluding a numerical solution in terms of the cooperative model described by eq 15 of McGhee & Von Hippel (1974), the intrinsic association constant to an isolated site may again be evaluated from the intercept on the axis of r/c (Crothers, 1968; Gurskii et al., 1972; McGhee & Von Hippel, 1974). The resulting value of $K_{(0)}$ for RNA contrasts with that found for DNA (Table II), revealing a 15-fold lower affinity for the ribose polymer. Raising the ionic strength of the buffer to 0.20 lowered binding constants generally but did not materially affect the shape of the Scatchard plots; again the data for RNA "mirrored" those for DNA (Figure 3b). However, the selectivity for DNA was enhanced to a value of 46-fold largely due to preferential reduction of the affinity for RNA (Table II). At even higher salt concentration the curvature of the Scatchard plot for DNA was much reduced (Figure 4b) such that the data were well fitted by eq 10 of McGhee & Von Hippel (1974), yielding binding parameters as listed in Table II. Thus it appears that binding to lower affinity sites, or the degree of anticooperativity between binding sites, is substantially reduced in high-salt buffer.

Table II: Binding Parameters for Crystal Violet–Nucleic Acid Interaction

nucleic acid	ionic strength	$K_{(0)}$ (M^{-1})	n^d	cooperativity parameter, ω
DNA[a]	0.01	1.5×10^5		
DNA[a]	0.20	1.6×10^4		
DNA[b]	0.75	3.1×10^3	4.5	
RNA[a]	0.01	1.0×10^4		>1
RNA[a]	0.20	3.5×10^2		>1
denatured DNA[c]	0.01	6.0×10^4	4.0	15.5
denatured DNA[c]	0.20	1.5×10^4	4.8	11

[a] Association constants determined by linear extrapolation of binding data to the Scatchard (1949) plot ordinate. [b] Determined by a nonlinear least-squares fit to eq 10 of McGhee & Von Hippel (1974). [c] Determined by a numerical solution to the cooperative eq 15 of McGhee & Von Hippel (1974). [d] Nucleotides per bound ligand molecule.

Heat denaturation of DNA profoundly affects its interaction with crystal violet (Figure 4a). The data now clearly exhibit the characteristic "humped" appearance of a cooperative process which is well described by eq 15 of McGhee & Von Hippel (1974). At low ionic strength (Figure 4a, circles), the cooperativity parameter (ω) is 15.5 and the binding constant falls between those determined for native DNA and RNA (Table II). However, at ionic strength 0.20 (Figure 4a, triangles), ω falls to 11 and the binding constant is 43-fold greater than that for RNA, though it is barely distinguishable from

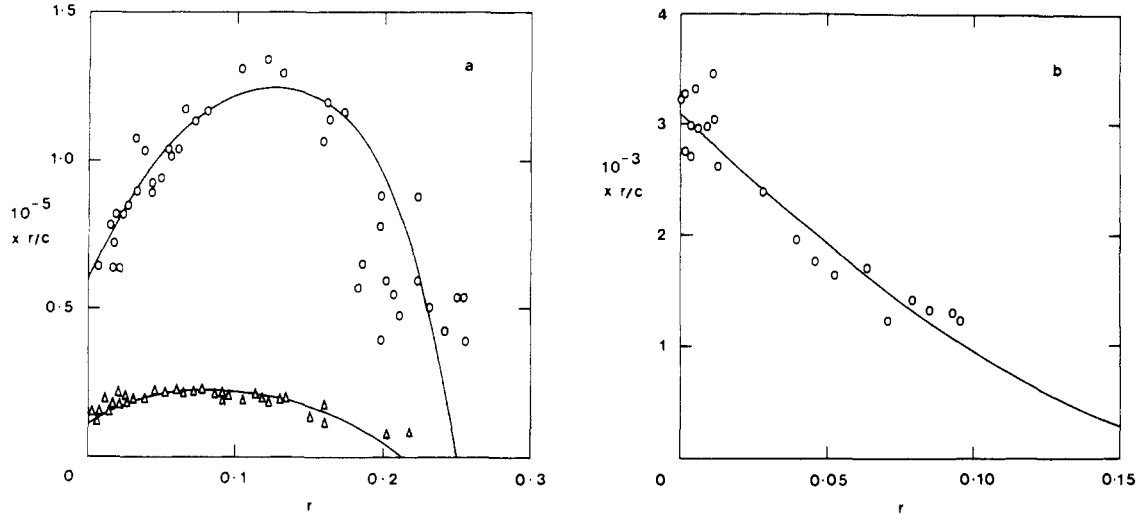

FIGURE 4: Scatchard plots for binding of crystal violet to heat-denatured DNA (a) and to native DNA at high ionic strength (b). (a) Heat-denatured calf thymus DNA in 0.01 SHE (○) and 0.20 SHE (△), pH 7.0, at 20 °C. The curves are theoretical, computed to fit eq 15 of McGhee & Von Hippel (1974) by using the values of $K_{(0)}$, ω, and n listed in Table II. (b) Native calf thymus DNA in buffer of ionic strength 0.75 and pH 6.0 at 25 °C. The curve is theoretical, computed to fit eq 10 of McGhee & Von Hippel (1974) by using the values of $K_{(0)}$ and n listed in Table II.

that determined for native DNA (Table II). The occluded binding site size for denatured DNA at both ionic strengths compares well with the value of 4.5 measured for native DNA at ionic strength 0.75 (Figure 4a,b, Table II).

The preferential binding to native DNA at low ionic strength is confirmed by the effect of crystal violet on the stability of calf thymus DNA toward thermal denaturation. Figure 5 shows that the ligand raises the melting temperature of native DNA by as much as 19 °C at the highest ratio studied (0.44), consistent with a substantially higher affinity for the double-helical form.

Spectroscopic Measurements. The temperature-jump difference spectra presented in Figure 6a show the total optical change accompanying the rise in temperature and therefore represent aggregate difference spectra between free and all the bound forms of crystal violet. At a binding ratio of 0.034 the difference spectrum recorded 1 ms after perturbing the temperature, when the transient had reached its equilibrium value (Figure 6a, circles), showed a peak at 540 nm and a trough at 610 nm, with an isosbestic point in the vicinity of 595–600 nm. Resolving the spectrum with respect to time at 510 nm, where the signal-to-noise ratio was greatest, revealed two fast closely coupled relaxation effects with time constants of 82 and 291 μs and amplitudes of 74.6 and 12.8 mV, respectively. Raising the DNA concentration to 1.5 mM and doubling the binding ratio to 0.070 produced the difference spectrum shown by the triangular symbols in Figure 6a, recorded at equilibrium 500 ms after the temperature jump. Although the central portion of the spectrum between 540 and 610 nm was obscured because of the high absorbance of the dye, it can be seen that the relative amplitudes and positions of the peaks were different. In particular, the negative peak shifted to longer wavelengths in the region 620–650 nm. The relaxation spectrum measured at 640 nm was found to comprise a total of four exponentials: the two closely coupled effects observed at the lower binding ratio, together with two slower, also closely coupled, relaxation times well separated from the fast effects. These latter components had relaxation times of 26.1 and 118.8 ms with amplitudes of 53.7 and 39.4 mV, respectively. Thus, at $r = 0.034$ crystal violet forms at least two distinct complexes with DNA whereas at $r = 0.070$ an additional two complexes can be detected, making a total of four distinct bound species at equilibrium. The difference

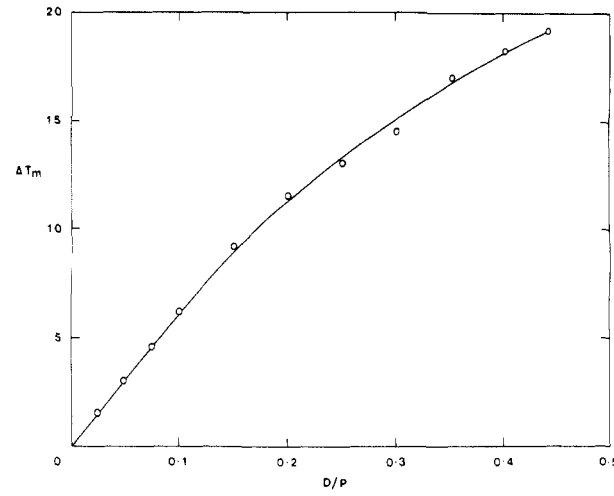

FIGURE 5: Effect of crystal violet on the thermal stability of calf thymus DNA. The ordinate shows the change in the midpoint of the hyperchromic transition compared with that of dye-free DNA (65 °C) in buffer of ionic strength 0.01. The abscissa shows the input ratio of dye molecules to DNA nucleotides.

spectrum of the high-r complex as presented in Figure 6a can largely be attributed to the optical properties of the slower equilibrating species whereas that of the low-r complex is characteristic of the faster binding processes.

Because of the evident complexity of the binding reaction revealed by the temperature-jump experiments, the spectral properties of bound crystal violet were further investigated as a function of binding ratio for DNA, RNA, and denatured DNA. Figure 6b records the visible absorption spectra at various levels of binding to calf thymus DNA in buffer of ionic strength 0.20. At very low r (≤ 0.0073) λ_{max} underwent a bathochromic shift from 590 to 595 nm, and the extinction coefficient was reduced by 5%. As the binding level rose, the peak continued to shift to longer wavelengths, finally reaching 600 nm at the highest value of r studied (0.059), where the hypochromicity increased to 26%. This behavior is atypical of intercalating agents but is reminiscent of that observed for the nonintercalating dye di-*tert*-butylproflavin (Müller et al., 1973). A dependence of the extinction coefficient of the bound dye on the degree of binding appears to be commonplace among A-T-specific ligands (Müller & Gautier, 1975).

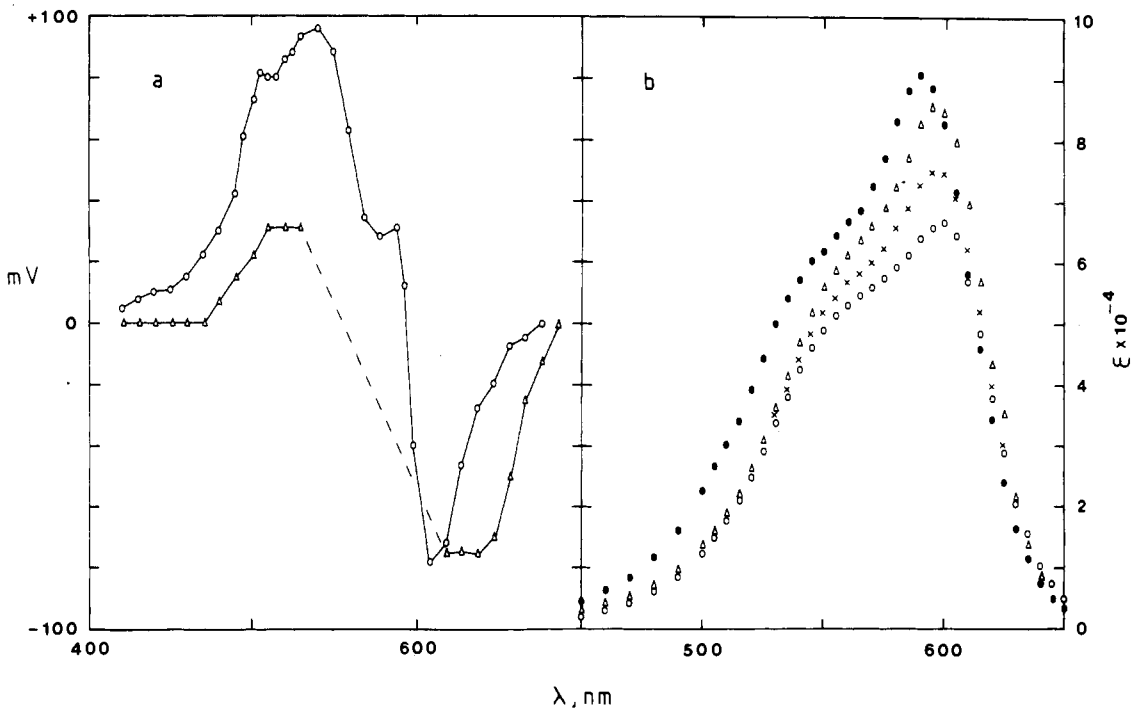

FIGURE 6: Temperature-jump difference spectra and visible absorption spectra of crystal violet bound to calf thymus DNA. (a) Temperature-jump difference spectrum measured in buffer of ionic strength 0.75 and pH 6.0 at 25 °C. Positive amplitudes represent an increase in absorbance. Symbols: (○) DNA concentration 1.0 mM, $r = 0.034$; (△) DNA concentration 1.5 mM, $r = 0.070$. (b) Visible absorption spectra measured in buffer of ionic strength 0.20 and pH 7.0 at 25 °C. Symbols: (●) free crystal violet; (△) $r = 0.007$; (×) $r = 0.041$; (○) $r = 0.059$.

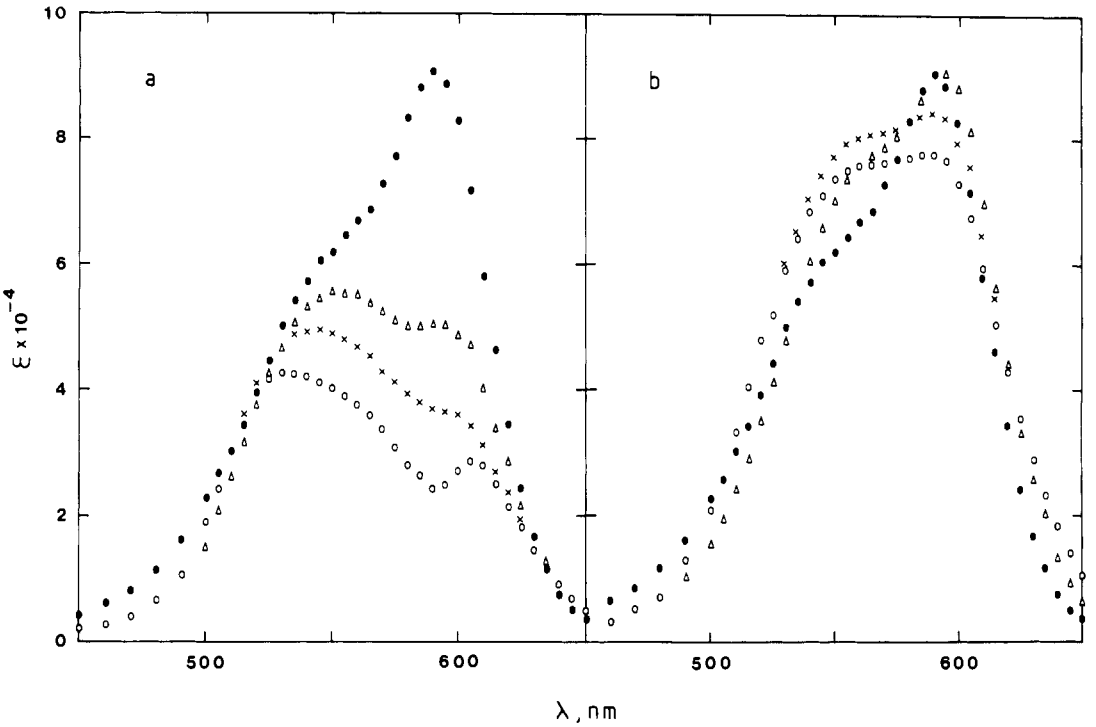

FIGURE 7: Visible absorption spectra of crystal violet bound to RNA (a) and heat-denatured DNA (b). All measurements were made in buffer of ionic strength 0.20 and pH 7.0 at 25 °C. Symbols in (a): (●) free crystal violet; (△) $r = 0.012$; (×) $r = 0.048$; (○) $r = 0.082$. Symbols in (b): (●) free crystal violet; (△) $r = 0.010$; (×) $r = 0.047$; (○) $r = 0.082$.

Comparison of the temperature-jump difference spectra in Figure 6a with the spectra presented in Figure 6b shows that following a temperature jump the binding equilibrium shifts so as to displace bound crystal violet, indicating that the enthalpy of reaction is negative.

The spectral changes associated with binding to RNA (Figure 7a) are quite different from those seen with DNA. Whereas with DNA the bound spectra retain the basic shape of the free ligand spectrum, on binding to RNA the shoulder at 550 nm in the free dye spectrum becomes the dominant peak and undergoes a hypsochromic shift; at the same time the maximum at 590 nm undergoes a bathochromic shift to 605 nm. As found for DNA there is progressive hypochromism with increasing r; here it is most marked at λ_{max} of the free dye (68% at $r = 0.082$).

With heat-denatured DNA the spectral properties of bound crystal violet appear different again and show less marked variation with the level of binding (Figure 7b). At higher r

there is a tendency for hypochromism at the major 590-nm peak, accompanied by augmentation of the shoulder at 550 nm, eventually resulting in one broad flat-topped absorption peak. Evidently the interaction of crystal violet with denatured DNA is characterized by complex spectral changes which do not relate monotonically to binding ratios but which, to some extent, resemble a mixture of weak spectral modifications like those observed on binding to native DNA and RNA.

Discussion

Sedimentation and Viscosity Measurements. The existence of multiple bound forms of crystal violet, so clearly emphasized by the spectroscopic and temperature-jump results, hampers interpretation of the experiments with circular DNA. At the equivalence binding ratio of 0.14 illustrated in Figures 1a and 2a,b, there appear to exist no less than four distinguishable bound species at equilibrium. It is not readily apparent how the helix-unwinding effect may be distributed among them. The problem is exacerbated by the result of the viscosity experiment with sonicated DNA which does not support a simple intercalative origin for the unwinding effect. Lacking further information, we can only state with certainty that the *average* value of the unwinding angle per bound dye molecule, 9.8°, is smaller than that commonly found for intercalating agents but is similar to that seen with steroidal diamines (Waring & Chisholm, 1972; Wakelin & Waring, 1974; Waring & Henley, 1975). The evidence suggests that steroidal diamines bind to kinks in DNA so as to promote local unstacking of the base pairs (Sobell et al., 1977; Dattagupta et al., 1978; Patel & Canuel, 1979). We must therefore consider the possibility that the apparent decrease in contour length observed for crystal violet complexes reflects bending of the helix as a result of ligand-induced kinking [see Reinert (1972), Balcarova et al. (1978), and Wakelin et al. (1978)]. This sort of effect would also account for the significant rise in the sedimentation coefficient of nicked circular molecules of PM2 DNA seen in Figure 1a. We can eliminate cross-linking by the dye as an explanation for this phenomenon since there was no evidence of aggregation of DNA molecules in the ultracentrifuge photographs.

It is, of course, possible that the measured reduction in contour length is not a consequence of bending but represents genuine shortening, for example, by ligand-induced transition from B-type to an A-type helical conformation. However, this mechanism would require that crystal violet bind with greater affinity to an A-type than to a B-type helix which is contrary to the findings of Müller & Gautier (1975): they reported a 10-fold lower binding constant for the mixed A-type polymer poly(rA)·poly(dT) compared with DNA. Their failure to find any effect of crystal violet on the contour length of DNA may be explained on the basis that their measurements were less sensitive to the influences of bending and/or kinking because their samples were sonicated to half the molecular weight of the preparation used here. Thus, the results of the hydrodynamic measurements are most consistent with a model in which crystal violet is bound externally to DNA, causing severe kinking and/or bending accompanied by a coupled unwinding of the Watson–Crick helix.

Equilibrium Binding Measurements. The marked curvature in the Scatchard plots for binding to DNA at low and moderate ionic strength accords with the notion that crystal violet has a general affinity for DNA superimposed upon a preferential interaction with some defined nucleotide sequence(s) (Müller & Gautier, 1975). Despite the uncertainty as to its mode of binding, the strength of interaction is impressive: $K_{(0)}$ for binding to an isolated site at ionic strength 0.01 is indistinguishable from that of the intercalating agent 9-aminoacridine and is only 3-fold lower than that of proflavin (Wilson et al., 1981). This contrasts with the 15-fold lower affinity of pararosaniline compared with proflavin (Armstrong & Panzer, 1972), again emphasizing the different character of the DNA complexes formed by these two triphenylmethane dyes (see the introduction). Although the shape of the Scatchard plot at high ionic strength suggests that binding of crystal violet to lower affinity sites is suppressed, it is clear from the temperature-jump measurements that there remain several bound forms. These latter measurements also support the view that the dye binds externally since the characteristics of its relaxation behavior are not typical of intercalation by either the sequential or the direct transfer mechanism (Li & Crothers, 1969; Bresloff & Crothers, 1975; Wakelin & Waring, 1980).

The totally different appearance of the equilibrium binding curves for DNA and RNA is a sure sign that the complexes formed with these nucleic acids are different. Whereas binding to DNA is subject to strong exclusion effects, binding to RNA is evidently a cooperative process. Attempts to determine whether crystal violet might bind preferentially to single-stranded or double-stranded regions in RNA by investigating its interaction with double-stranded poly(rA)·poly(rU) were frustrated by precipitation of the complex even at very low polynucleotide concentrations. Thus we can only speculate as to the origins of the cooperativity, and it remains as yet undetermined whether the dye binds preferentially to single- or double-stranded regions of RNA. Were the former situation to prevail, then a ligand-induced conformational transition from hairpin helical to single-stranded RNA would provide the basis for cooperativity. Another notable difference from the interaction of crystal violet with DNA lies in the extreme sensitivity of the RNA complex to increases in ionic strength. Thus, on raising the salt concentration from 0.01 to 0.20 M the affinity for RNA is lowered 29-fold whereas the binding constant for DNA drops only 10-fold. This could mean that the RNA complex is stabilized to a larger extent by electrostatic forces than is the case for the DNA complex. On the other hand, it might reflect the propensity of the higher ionic strength medium to promote double strandedness in the polymer which, if the dye binds preferentially to single-stranded RNA, would also result in reduced binding.

With heat-denatured DNA we may reasonably presume that the dye binds preferentially to residual helical regions, if only because it strongly stabilizes native DNA against thermal denaturation (Figure 5). Thus in this instance the observed cooperativity of binding can be attributed to ligand-induced stabilization of double-stranded regions in the denatured polymer. This interpretation is supported by the ionic strength dependence of the binding parameters, since the affinity for denatured DNA drops by a factor of only 4 on raising the salt concentration from 0.01 to 0.20 M (cf. the 10- and 29-fold reductions for native DNA and RNA, respectively) and the cooperativity parameter is reduced from 16 to 11. When the expected reduction in the electrostatic contribution to the free energy of binding caused by raising the ionic strength is borne in mind, these changes are consistent with selective binding to the increased proportion of double-helical regions favored in the high-salt buffer. Furthermore, this hypothesis can also account for the similarity in the intrinsic affinities of crystal violet for native and denatured DNA at ionic strength 0.2.

Spectroscopic Measurements. NMR and spectroscopic studies have indicated that the 550-nm shoulder in the visible absorption spectrum of aqueous solutions of crystal violet

should be attributed to the presence of aggregated dye molecules (Barker et al., 1959; Schuster et al., 1968). These studies also showed that twisting the phenyl rings about the central carbon atom and similarly reducing conjugation of the dimethylamino groups with the phenyl rings both cause bathochromic and hypochromic shifts which are related to the degree of deformation of the symmetrical propeller structure (Barker et al., 1959, 1960). Thus, the variations in the absorption spectrum of bound crystal violet may provide information concerning both the relative disposition of the phenyl and dimethylamino groups and the extent of aggregation of ligand molecules in the dye–nucleic acid complex. One notable feature in all spectra of bound crystal violet is the presence, and indeed prominence in the case of RNA, of the 550-nm shoulder. This suggests that even at very low levels of binding ($r \leq 0.01$) the ligand forms aggregates on the surface of the polynucleotide, especially with those nucleic acids which display cooperative behavior. Although hypochromic and bathochromic shifts are commonly observed in ligand–DNA interactions, the binding level dependence of these changes in the spectrum of DNA-bound crystal violet speaks for progressive moderate rotation either of the phenyl rings about the central carbon or of the dimethylamino groups out of the aromatic planes as the lattice becomes more saturated (Barker et al., 1959, 1960). By contrast, in the crystal violet–RNA spectra, not only is there greater evidence of aggregation but also the marked hypochromicity is more characteristic of perturbation of the dimethylaminophenyl ring resonance (Barker et al., 1959, 1960). Thus while the detailed character of crystal violet–nucleic acid interaction remains to be elucidated at the molecular level, the present results clearly confirm the dependence of the structure of the complex on the type of polynucleotide as well as on the level of binding. Further studies employing other optical and spectroscopic techniques, especially with synthetic polynucleotides, are expected to throw light on these outstanding problems.

References

Armstrong, R. W., & Panzer, N. M. (1972) *J. Am. Chem. Soc. 94*, 7650–7653.

Balcarova, Z., Kleinwächter, V., Koudelka, J., Löber, G., Reinert, K. E., Wakelin, L. P. G., & Waring, M. J. (1978) *Biophys. Chem. 8*, 27–40.

Barker, C. C., Bride, M. H., & Stamp, A. (1959) *J. Chem. Soc.* 3957–3963.

Barker, C. C., Hallas, G., & Stamp, A. (1960) *J. Chem. Soc.* 3790–3800.

Bresloff, J. L., & Crothers, D. M. (1975) *J. Mol. Biol. 95*, 103–123.

Cohen, G., & Eisenberg, H. (1966) *Biopolymers 4*, 429–440.

Cohen, G., & Eisenberg, H. (1969) *Biopolymers 8*, 45–55.

Crothers, D. M. (1968) *Biopolymers 6*, 575–584.

Crothers, D. M., & Zimm, B H. (1965) *J. Mol. Biol. 12*, 525–536.

Dattagupta, N., Hogan, M., & Crothers, D. M. (1978) *Proc. Natl. Acad. Sci. U.S.A. 75*, 4286–4290.

Espejo, R. T., Canelo, E. S., & Sinsheimer, R. L. (1969) *Proc. Natl. Acad. Sci. U.S.A. 63*, 1164–1168.

Farnum, D. G. (1964) *J. Am. Chem. Soc. 86*, 934–935.

Farnum, D. G. (1967) *J. Am. Chem. Soc. 89*, 2970–2975.

Gomes de Mesquita, A. H., MacGillavry, C. H., & Eriks, K. (1965) *Acta. Crystallogr. 18*, 437–443.

Gurskii, G. V., Zasedatelev, A. S., & Vol'kenshtein, M. V. (1972) *Mol. Biol. (Engl. Transl.) 6*, 429–490.

Johnson, M. L., & Schuster, T. M. (1974) *Biophys. Chem. 2*, 32–41.

Keller, W. (1975) *Proc. Natl. Acad. Sci. U.S.A. 72*, 4876–4880.

Lee, J. S., & Waring, M. J. (1978) *Biochem. J. 173*, 115–128.

Lerman, L. S. (1961) *J. Mol. Biol. 3*, 18–30.

Lerman, L. S. (1964a) *J. Cell. Comp. Physiol., Suppl. 1 64*, 1–18.

Lerman, L. S. (1964b) *J. Mol. Biol. 10*, 367–380.

Li, H. J., & Crothers, D. M. (1969) *J. Mol. Biol. 39*, 461–477.

McGhee, J. D., & Von Hippel, P. H. (1974) *J. Mol. Biol. 86*, 469–489.

Moodie, R. B., Connor, T. M., & Stewart, R. (1959) *Can. J. Chem. 37*, 1402–1408.

Müller, W., & Crothers, D. M. (1968) *J. Mol. Biol. 35*, 251–290.

Müller, W., & Gautier, F. (1975) *Eur. J. Biochem. 54*, 385–394.

Müller, W., Crothers, D. M., & Waring, M. (1973) *Eur. J. Biochem. 39*, 223–234.

Neville, D. M., & Davies, D. R. (1966) *J. Mol. Biol. 17*, 57–74.

Olah, G. A. (1964) *J. Am. Chem. Soc. 86*, 932–934.

Patel, D. J., & Canuel, L. L. (1979) *Proc. Natl. Acad. Sci. U.S.A. 76*, 24–28.

Ray, G. J., Kurland, R. J., & Colter, A. K. (1971) *Tetrahedron 27*, 735–752.

Reinert, K. E. (1972) *J. Mol. Biol. 72*, 593–607.

Revet, B. M. J., Schmir, M., & Vinograd, J. (1971) *Nature (London), New Biol. 229*, 10–13.

Scatchard, G. (1949) *Ann. N.Y. Acad. Sci. 51*, 660–672.

Schuster, I. I., Colter A. K., & Kurland, R. J. (1968) *J. Am. Chem. Soc. 90*, 4679–4687.

Sobell, H. M., Jain, S. C., Tsai, C., & Gilbert, S. G. (1977) *J. Mol. Biol. 114*, 333–365.

Wakelin, L. P. G. & Waring, M. J. (1974) *Mol. Pharmacol. 10*, 544–561.

Wakelin, L. P. G., & Waring, M. J. (1976) *Biochem. J. 157*, 721–740.

Wakelin, L. P. G., & Waring, M. J. (1980) *J. Mol. Biol. 144*, 183–214.

Wakelin, L. P. G., Romanos, M., Chen, T. K., Glaubiger, D., Canellakis, E. S., & Waring, M. J. (1978) *Biochemistry 17*, 5057–5063.

Wang, J. C. (1974) *J. Mol. Biol. 89*, 783–801.

Waring, M. J. (1970) *J. Mol. Biol. 54*, 247–279.

Waring, M. J., & Chisholm, J. W. (1972) *Biochim. Biophys. Acta 262*, 18–23.

Waring, M. J., & Wakelin, L. P. G. (1974) *Nature (London) 252*, 653–657.

Waring, M. J., & Henley, S. M. (1975) *Nucleic Acids Res. 2*, 567–586.

Wilson, W. R., Baguley, B. C., Wakelin, L. P. G., & Waring, M. J. (1981) *Mol. Pharmacol.* (in press).